Partially penetrating slug tests in an unweathered till layer

David W. Ostendorf, William G. Lukas and Don J. DeGroot

ABSTRACT

This research improves field based estimates of aquitard compressibility and permeability. A semianalytical model of partially penetrating, overdamped slug tests achieves this objective. The short term solution is an existing fully penetrating model, the long term solution is the polar residue of an inverse Laplace transform, and an exponential spline function patches the solutions together. Large amplitude slug test data from ten pairs of partially penetrating monitoring wells installed in an unweathered till at Scituate Hill in eastern Massachusetts calibrate the model. The deposit is bound by weathered till and the Dedham Granite fracture zone, and both are far more permeable than the unweathered till. The calibrated till permeability of 8.4×10^{-16} m^2 is about 25% less than existing model calibrations that include boundary recharge in permeability values. The calibrated till compressibility of 5.1×10^{-10} Pa^{-1} reflects the proper inclusion of recharge as a long term source of groundwater, rather than the unrealistically large compressibility calibrations required by fully penetrating models.

Key words | drumlin, glacial till, groundwater, slug tests

David W. Ostendorf (corresponding author)
William G. Lukas
Don J. DeGroot
Civil and Environmental Engineering Department,
University of Massachusetts,
Amherst,
MA 01003,
USA
E-mail: *dostendo@umass.edu*

NOMENCLATURE

A_J	Jth Fourier sine series coefficient (m-s)
a_0	simple pole (1/s)
B_J	integrating factor of Jth sine series coefficient
b	unweathered till thickness (m)
c_J	Jth integration constant (m-s)
D	hydraulic diffusivity (m^2/s)
F_{Short}	transform of short term solution (m-s)
$f(t)$: $F(p)$	Laplace transform pair
g	gravitational acceleration (m/s^2)
H_O	amplitude of slug test (m)
h	disturbed hydraulic head (m)
h_{Long}	long term solution for disturbed water level in well (m)
h_{Res}	residue of simple pole (m)
h_S	disturbed water level in well (m)
h_{Short}	short term solution for disturbed water level in well (m)
h^*	transformed hydraulic head (m-s)
h_S^*	transformed hydraulic head in well (m-s)
J_N	Bessel function of the first kind, of order N
K_N	modified Bessel function of the second kind, of order N
k	permeability of unweathered till (m^2)
k_{BR}	Bouwer & Rice (1976) estimate of unweathered till permeability (m^2)
L	length of sandpack (m)
L_{Match}	matching length (m)
m_J	Jth radial eigenfunction (m-s)
p	Laplace transform variable (1/s)
p_{Gage}	gage pressure (kg/m-s^2)
q_J	Jth vertical eigenfunction
R	distance along negative real axis of Bromwich contour (1/s)
R_J	Jth branch point (1/s)
r	radial distance from center of well (m)

doi: 10.2166/nh.2016.159

r_C radius of casing (m)
r_e effective radius in Bouwer & Rice (1976) model (m)
r_S radius of sandpack (m)
S unweathered till storativity
T unweathered till transmissivity (m^2/s)
t time from start of slug test (s)
u changed variable of integration in Cooper *et al.* (1967) model
Y_N Bessel function of the second kind, of order N
z elevation above lower recharge boundary (m)
z_S elevation of the base of the sandpack (m)
z_T elevation of transducer (m)
α unweathered till compressibility ($m\text{-}s^2/kg$)
β sum of integrating factors
ρ density of groundwater (kg/m^3)
ν kinematic viscosity of groundwater (m^2/s)

INTRODUCTION

We derive and calibrate a closed form model of partially penetrating slug tests to improve field based estimates of aquitard compressibility and permeability. Aquitards are important because they protect underlying aquifers from surface contamination (van der Kamp 2001), an attribute of particular significance in stratified drift deposits (Klinger 1996) and till mantled bedrock (Lukas *et al.* 2015) of New England. Aquitard leakage affects confined aquifer hydraulics (Wang *et al.* 2015), and an improved understanding of the confining layer properties distinguishes recharge from aquifer compressibility in the calibration of transient pump test data (Neuman & Witherspoon 1969).

Slug tests estimate hydraulic properties of soil near monitoring wells, as documented by an established (Butler 1997) and continuing (Sakata *et al.* 2015) literature. Impermeable soil responds monotonically to an abrupt change of head in the well, and Cooper *et al.* (1967) use Laplace transforms to derive an analytical model for a fully penetrating sandpack in a confined aquifer. The overdamped slug test theory balances radial flow and storage in the soil with an integrated conservation of mass for the monitoring well imposed as a boundary condition at the interface of the sandpack and soil. Water level observations in the well calibrate the aquifer transmissivity and storativity, hence the radial permeability and compressibility of the soil. Partially penetrating wells, packers, or unconfined aquifers add a vertical component to the hydraulics of overdamped slug tests (Zlotnik 1994). Bouwer & Rice (1976) neglect soil storage, and compare cylindrical finite difference solutions with a radial closed form solution for overdamped slug tests in an unconfined aquifer to determine an equivalent radius in the soil. The latter determines the exponential decay constant for the water level in the monitoring well, along with the calibrated soil permeability. Hvorslev (1951) adopts a similar approach, but uses a steady cylindrical solution and shape factors to infer soil permeability from an exponential decay constant. Hyder *et al.* (1994) include soil storage in their cylindrical model of overdamped slug test hydraulics and derive a closed form Laplace transform solution for partially penetrating wells in a confined aquifer. Their transformed solution is inverted numerically, and features in many recent investigations. Paradis & Lefebvre (2013) use it to interpret slug test data in observation and slugged intervals in a single monitoring well equipped with multiple packers. Brauchler *et al.* (2010) use the Hyder *et al.* (1994) model to interpret slug test data in separate observation wells. Yeh *et al.* (2008) add a skin zone to the cylindrical model of a partially penetrating slug test in a confined aquifer and, like Hyder *et al.* (1994), invert the analytical Laplace transform solution numerically. Multiple wells and more complicated groundwater settings require numerical models, and Yang *et al.* (2015) summarize a recent MODFLOW application in aquitards. The challenge of heterogeneous property estimation from an array of observation and partially penetrating slugged wells is considered as an inverse tomographic exercise by Paradis *et al.* (2015).

Our study was motivated by the documented response of unweathered till monitoring wells to the introduction of seasonal pumping from underlying fractured bedrock more than a decade after the initial site characterization experiments. The latter followed van der Kamp's (2001) strategy of aquitard analysis across steady, seasonal, and diurnal scales; and included Hvorslev (1951) permeability calibration of slug tests and downward attenuation of

storm scale transience for compressibility estimation (Ostendorf *et al.* 2004). Bedrock pumping introduces seasonal transience from below, and reveals the fracture zone as a leaky aquifer (Hantush 1960). Discrete (Ostendorf *et al.* 2015a) and continuous (Lukas *et al.* 2015) records of drawdown and recovery in the monitoring wells calibrate site averaged values for permeability and compressibility of the till. Ostendorf *et al.* (2015b) confirm the corresponding bedrock properties with a novel theory of slug tests and geophysical logs in uncased boreholes through the fracture zone. The present study completes the cycle in the till, with an improved model of partially penetrating slug tests that includes compressibility and recharge boundaries.

SITE DESCRIPTION

Scituate Hill

The theory is used to calibrate unweathered till properties at a well characterized field site in eastern Massachusetts (Figure 1). The site is a Massachusetts Department of Transportation highway deicing agent storage facility built in the 1960s on Scituate Hill, a glacial lodgment till drumlin in Cohasset (Ostendorf *et al.* 2004). The ground surface is about 55 m above mean sea level (mmsl), the water table is about 50 mmsl and occurs in a weathered till about 8 m thick, which overlies the unweathered till at about 45 mmsl. Soil moisture and grain size distributions from split spoon samples obtained during monitoring well construction suggest that the till is well graded and uniformly dense with an average porosity of 22%. Typical average particle size fractions are 17% gravel, 39% sand, 33% silt and 11% clay. Nearby excavations suggest cobbles and boulders are also present. The unweathered till in turn overlies the fracture zone of the Dedham Granite (Goldsmith 1991) with a contact surface at about 15 mmsl in the study area. Thus the unweathered till thickness b is set equal to 30 m, as cited in Table 1, which summarizes adopted and calibrated parameter values site wide.

Prior testing, modeling, and analysis have established that the weathered till and bedrock fracture zones are more than an order of magnitude more permeable than the unweathered till between them. Infiltration and unconfined aquifer hydraulics at steady and seasonal scales have established weathered till permeability of $10^{-13}\,m^2$ in radial (Ostendorf *et al.* 2004) and horizontal (Ostendorf *et al.* 2015a) flow fields along the toe and flank of the drumlin. Irrigation pumping from the Dedham Granite at an adjacent apartment complex completed in 2011 has revealed the fracture zone hydraulics to function as a confined aquifer of $4\times10^{-5}\,m^2/s$ transmissivity that receives leakage from the unweathered till.

Monitoring well details and slug test protocol

Twenty-two monitoring well clusters were constructed by the University of Massachusetts Amherst in the late 1990s and early 2000s to investigate the fate, transport, and remediation of deicing agent chloride contamination of the groundwater (Ostendorf *et al.* 2006). Ten of the clusters include pairs of 0.025 m radius (r_C) PVC monitoring wells, with 1.52 m screen sections with uniform sandpacks in closely spaced (<5 m) boreholes. One well was drilled to the contact surface with the Dedham Granite and a second was drilled 15–25 m higher up in the unweathered till. Table 2 lists attributes of the pairs, which feature sandpack radii r_S varying from 0.049 to 0.108 m and sandpack lengths L from 2.13 to 2.74 m in extent, and, in one instance, 5.34 m. The sandpacks were sealed with bentonite grout or chips, and each monitoring well was finished with a locked steel cover and concrete collar at the ground surface.

Slug tests were conducted in the winter of 2013 and the summer of 2015. The water level was measured manually in the well prior to purging with an electronic meter (Slope Indicator, Seattle, WA, USA) in order to confirm the elevation z_T of a piezoresistive pressure transducer (In Situ, Fort Collins, CO, USA) above the cluster interface with the Dedham Granite (Table 2). The transducer was removed briefly (<10 minutes) while a Waterra purge pump (New England Environmental, Waltham, MA, USA) evacuated the monitoring well in order to establish the amplitude of the slug test. The transducer was then reinserted into the monitoring well and the subsequent recovery of head in the well logged at 15 minute intervals.

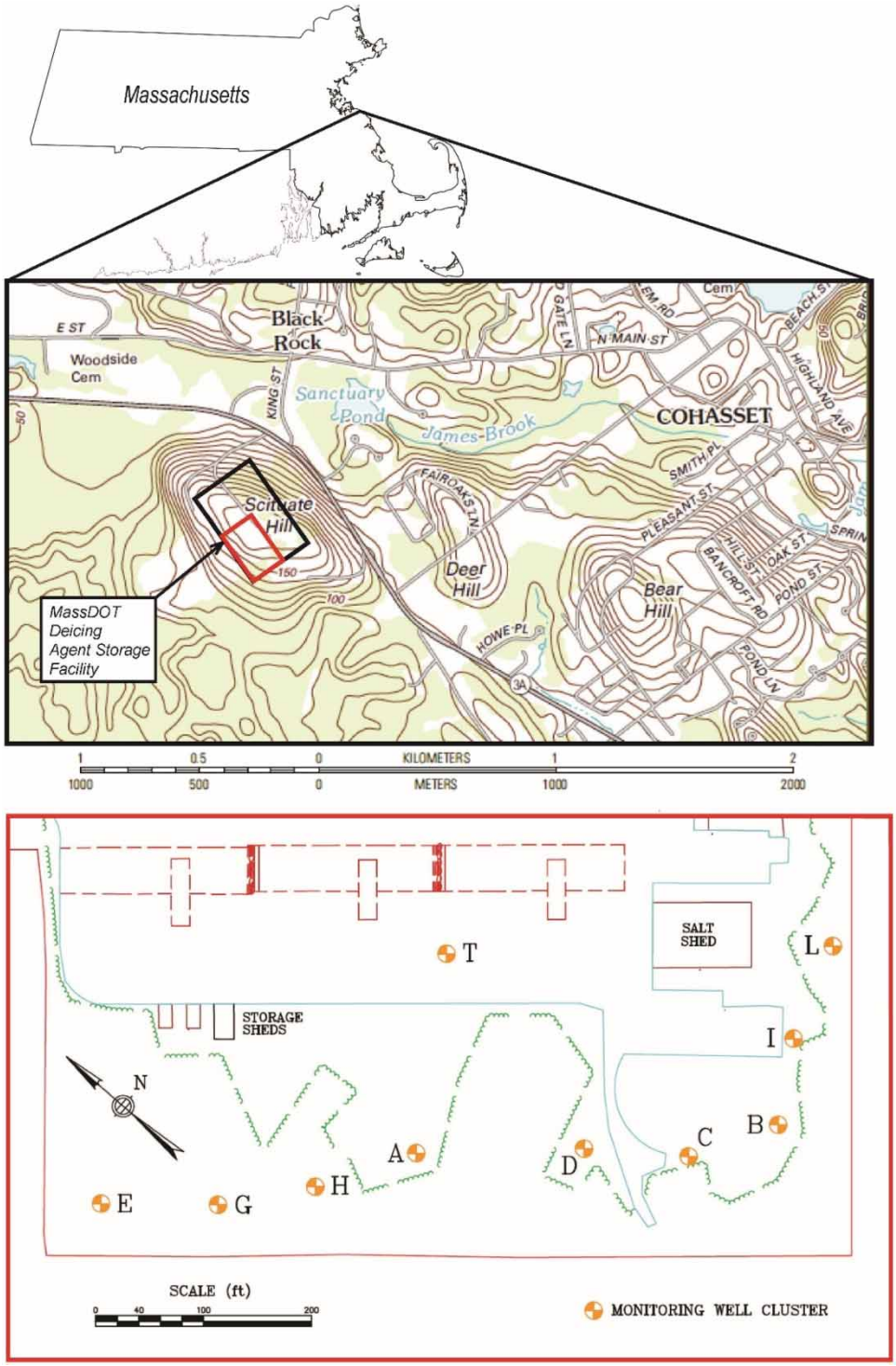

Figure 1 | MassDOT highway deicing agent storage facility and UMass monitoring well clusters.

Table 1 | Adopted and calibrated parameter values

Parameter	Value	Source
Unweathered till thickness (b)	30 m	Soil borings
Groundwater kinematic viscosity (ν)	1.3×10^{-6} m^2/s	White (2011)
Groundwater density (ρ)	1.0×10^{3} m^3/s	White (2011)
Weathered till permeability	10^{-13} m^2	Ostendorf *et al.* (2004)
Leaky bedrock aquifer transmissivity	4×10^{-5} m^2/s	Ostendorf *et al.* (2015a)
Casing radius (r_C)	2.5 cm	Ostendorf *et al.* (2004)
Unweathered till permeability (k)	8.4×10^{-16} m^2	Geometric calibration average
Unweathered till compressibility (α)	5.1×10^{-10} Pa^{-1}	Arithmetic calibration average
Matching length (L_{Match})	6.3 m	Arithmetic calibration average

Table 2 | Monitoring well geometry and slug test conditions

Well (date)	r_S, m	L, m	z_S, m	β	z_T, m	H_O, m
AB (1/29/13)	0.108	2.59	0.0	0.086	1.1	–21.0
AD (7/28/15)	0.049	2.13	18.5	0.070	18.8	–8.88
BB (7/28/15)	0.108	1.89	16.9	0.062	17.5	–7.17
BC (1/29/13)	0.108	2.59	0.0	0.086	6.4	–22.3
CB (1/29/13)	0.108	2.44	0.0	0.082	1.8	–23.0
CD (7/28/15)	0.108	2.13	20.2	0.070	20.5	–7.19
DB (1/29/13)	0.108	2.13	0.0	0.070	3.7	–25.3
DC (7/28/15)	0.108	2.13	21.8	0.070	21.9	–7.66
EB (8/4/15)	0.108	2.21	0.0	0.072	0.3	–15.6
ED (7/28/15)	0.108	2.44	16.7	0.082	17.4	–10.4
GB (1/29/13)	0.049	5.34	0.0	0.18	1.0	–18.6
GC (7/28/15)	0.049	2.13	18.0	0.070	18.9	–7.46
HB (1/29/13)	0.049	2.44	0.0	0.082	0.7	–19.6
HC (7/28/15)	0.049	2.59	18.9	0.086	20.7	–7.08
IB (1/29/13)	0.108	2.13	0.0	0.070	0.1	–24.0
ID (7/28/15)	0.108	2.44	25.9	0.081	26.2	–6.41
LA (1/29/13)	0.108	2.13	0.0	0.070	14.5	–26.5
LD (7/28/15)	0.108	2.44	21.7	0.070	23.0	–8.78
TA (8/4/15)	0.049	2.74	0.0	0.090	1.0	–19.3
TD (7/28/15)	0.049	2.44	16.1	0.081	16.6	–10.0

The gage pressure p_{Gage} sensed by the vented transducer estimates the disturbed head measured in the well:

$$h_S(measured) = H_O + \frac{p_{Gage}}{\rho g} + z_T \; (H_O < 0) \tag{1}$$

The groundwater density is ρ and gravitational acceleration is g.

Modifications for the study site

Our study site featured large amplitude, partially penetrating slug tests in an aquitard with permeable boundaries, so the existing aquifer theory had to be modified to calibrate the results. Figure 2 shows disturbed water levels h_S observed in monitoring wells AB and HB. The wells were pumped dry at time t equals zero, so that the slug test amplitude H_O was negative and large, with absolute values in excess of 20 m at the start of the tests. Semilog plots of the first 150 hours suggest that AB was far less permeable than HB, as the levels decreased by an order of magnitude in 3 days and 5 hours, respectively (Figure 2(a) and 2(b)), followed by a slower decrease from 1 m to centimeter scale disturbances (Figure 2(c) and 2(d)). The asymptotic approach to straight lines in the semilogarithmic Figure 2(a) and 2(b) does imply exponential late term behavior, as is also predicted by Bouwer & Rice (1976). Figure 2(c) and 2(d) suggest that the slope of the regression is distorted by ambient transience at the centimeter scale, however. Figure 2(e) and 2(f) are linear plots of the last 150 hours of both tests. The monitoring wells recovered hydraulic heads above their starting levels at the end of the tests, implying a seasonal rise of head due to recharge and cessation of irrigation pumping adjacent to the site (Ostendorf *et al.* 2015a). Aperiodic storm scale transience appeared at the 230–260-hour intervals in both wells, and a semidiurnal earth tide was easily seen in well HB, due to its proximity to underlying permeable bedrock. Our use of large amplitude slug tests adds a second order of magnitude to the data before distortion by earth tides, barometric pressure fluctuations, recharge, and pumping disturbances.

The exact integration of the Bromwich contour needed to invert transformed cylindrical hydraulics is complicated, as demonstrated by Neuman & Witherspoon (1969) for

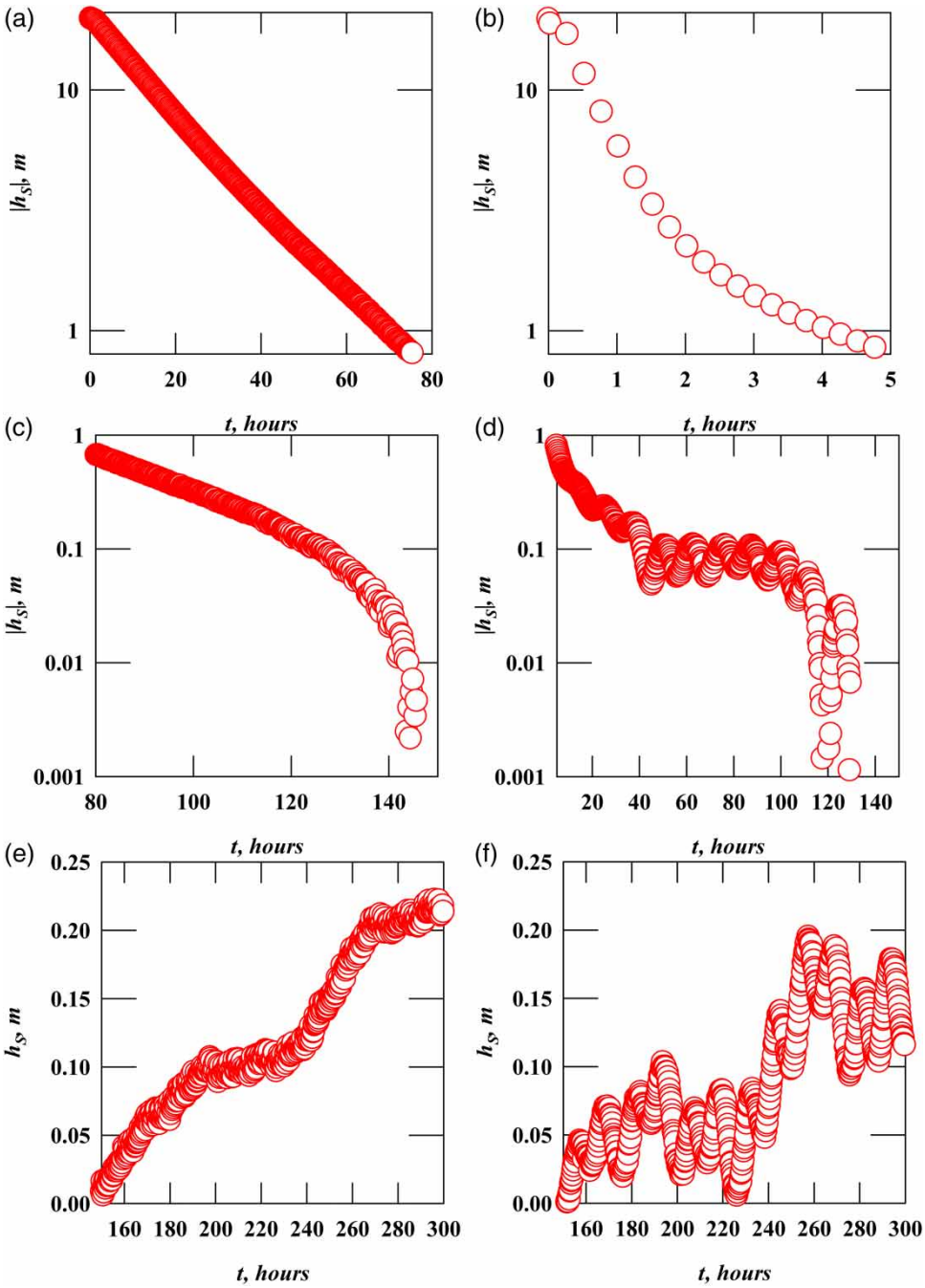

Figure 2 | Semilogarithmic and linear plots of disturbed head observed during (a), (c), (e) slug test AB and (b), (d), (f) slug test HB.

pump tests in leaky aquifers. We follow Hantush (1960) instead, who interpolates between simple short and long term solutions in his analysis of pump tests in leaky aquifers. Our long term solution is exponential, with a pole and a residue that permit a semilogarithmic regression whose slope and intercept calibrate the compressibility and permeability of the unweathered till. The short term solution is similar to that of Cooper *et al.* (1967), with the inclusion of a factor dependent on partial well geometry. Our closed form model, though new, does rest on its predecessors.

MATHEMATICAL MODEL

Governing equation and assumed transformed solution for cylindrical flow

The conservation of incompressible groundwater mass and Darcy's law describe the disturbed hydraulic head h in a confined, homogeneous, isotropic till of compressibility α:

$$\frac{\partial h}{\partial t} - D\left[\frac{1}{r}\frac{\partial}{\partial r}\left(r\frac{\partial h}{\partial r}\right) + \frac{\partial^2 h}{\partial z^2}\right] = 0 \tag{2a}$$

$$D = \frac{k}{\rho v \alpha} \tag{2b}$$

$$h = 0\,(t = 0) \tag{2c}$$

$$h = 0\,(z = 0; z = b) \tag{2d}$$

$$h = 0\,(r \to \infty) \tag{2e}$$

$$\pi r_C^2 \frac{\partial h}{\partial t} = \frac{2\pi k g r}{v} \int_{z_S}^{z_S+L} \frac{\partial h}{\partial r} dz \;\; (r = r_S, z_S < z < z_S + L) \tag{2f}$$

$$h = H_O \;\; (t = 0,\; r = r_S,\; z_S < z < z_S + L) \tag{2g}$$

with radial distance r from the axis of a well and elevation z above the lower recharge boundary, and elevation of the base of the sandpack z_S (Figure 3). The permeability k combines with ρ and kinematic viscosity v of the groundwater to define a hydraulic diffusivity D. These properties describe the propagation of disturbances caused by an overdamped slug test in a well that partially penetrates the till.

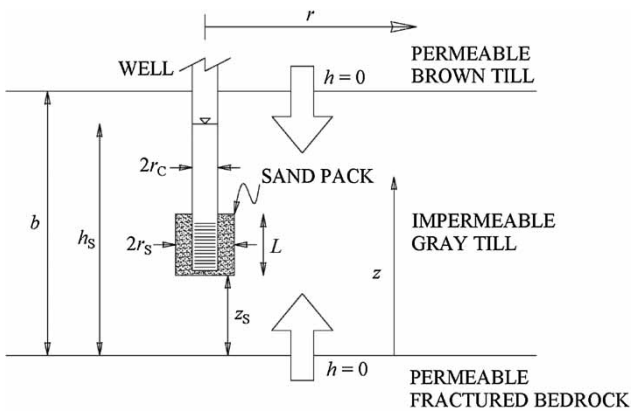

Figure 3 | Definition sketch, with recharge layer and till labels for the field research site.

The disturbed hydraulic head is zero initially in the till and at the boundaries of the recharge layers that bound the till. The spatial dependence is then separable and linear. The Laplace transform h^* of Equations (2a) and (2c) is thus the sum of vertical $q_J(z)$ and radial $m_J(r)$ eigenfunctions, each governed by an ordinary, second order differential equation:

$$h* = \sum_{J=1}^{\infty} q_J(z) m_J(r) \tag{3a}$$

$$p - D\left[\frac{1}{r m_J}\frac{d}{dr}\left(r\frac{dm_J}{dr}\right) + \frac{1}{q_J}\frac{d^2 q_J}{dz^2}\right] = 0 \tag{3b}$$

The Laplace transform variable is p. Boundary conditions constrain the eigenfunctions by distinguishing their type and integration constants.

We assume a finite vertical length scale imposed by the unweathered till thickness. A Fourier sine series solution satisfies the Laplace transform of the no head conditions (2d) at the two horizontal recharge boundaries:

$$q_J = sin\left(\frac{J\pi z}{b}\right) \tag{4}$$

Equations (3) and (4) imply a Bessel function solution for the radial eigenfunctions (Hildebrand 1976). The transience dies out with increasing radial distance when Equation (2e) is transformed, so that N order modified Bessel functions of the second kind K_N are chosen for m_J:

$$m_J = c_J K_0\left(\frac{r}{\sqrt{D}}\sqrt{p + R_J}\right) \tag{5a}$$

$$R_J = D\left(\frac{J\pi}{b}\right)^2 \tag{5b}$$

Branch points R_J are defined for each eigenfunction. The transformed solution is:

$$h* = \sum_{J=1}^{\infty} c_J K_0\left(\frac{r}{\sqrt{D}}\sqrt{p + R_J}\right) sin\left(\frac{J\pi z}{b}\right) \tag{6}$$

The solution approaches a vertically uniform transformed head h_S^* at the sandpack radius over the sandpack length, and vanishes elsewhere as the radius goes to zero:

$$h^* = h_S^* \ (r = r_S, z_S < z < z_S + L) \tag{7a}$$

$$h^* = 0 \ (r = r_S \ z < z_S, z_S + L < z < b) \tag{7b}$$

Equations (6) and (7) may be taken as a Fourier sine series representation of a boxcar function over the till thickness. Hildebrand (1976) evaluates the series coefficients A_J:

$$A_J = \frac{2h_S^*}{b} \int_{z_S}^{z_S+L} sin\left(\frac{J\pi z}{b}\right) dz \tag{8a}$$

$$A_J = 2h_S^*(p) B_J \tag{8b}$$

$$B_J = \frac{\cos\left(\frac{J\pi z_S}{b}\right) - cos\left[\frac{J\pi(z_S+L)}{b}\right]}{J\pi} \tag{8c}$$

The coefficients B_J reflect the partial penetration of the sandpack. In view of Equations (6) and (8), the integration constants c_J depend on h_S^*:

$$c_J = h_S^* \frac{2B_J}{K_0\left(\frac{r_S}{\sqrt{D}}\sqrt{p+R_J}\right)} \tag{9a}$$

$$h^* = h_S^* \sum_{J=1}^{\infty} \frac{2B_J K_0\left(\frac{r}{\sqrt{D}}\sqrt{p+R_J}\right)}{K_0\left(\frac{r_S}{\sqrt{D}}\sqrt{p+R_J}\right)} sin\left(\frac{J\pi z}{b}\right) \tag{9b}$$

The Laplace transform of the slug test condition, Equations (2f) and (2g), is:

$$ph_S^* - H_O = \frac{2kgr}{\nu r_C^2} \int_{z_S}^{z_S+L} \frac{dh^*}{dr} dz \ (r = r_S) \tag{10}$$

Equation (9b) is differentiated term by term with respect to r and evaluated at the sandpack radius. The result is solved for h_S^*:

$$h_S^* = \frac{H_O}{p + \frac{4T}{r_C^2} \sum_{J=1}^{\infty} B_J^2 \frac{r_S}{\sqrt{D}}\sqrt{p+R_J} \frac{K_1\left(\frac{r_S}{\sqrt{D}}\sqrt{p+R_J}\right)}{K_0\left(\frac{r_S}{\sqrt{D}}\sqrt{p+R_J}\right)}} \tag{11a}$$

$$T = \frac{kgb}{\nu} \tag{11b}$$

Equation (11b) defines the transmissivity T.

Short term solution

Hantush (1960), faced with a complicated transformed solution for leaky aquifer drawdown, argues that the initial behavior can be deduced by inverting the transformed solution for large p. The logic is applied to Equation (11a) with the limiting result:

$$h_S^* = \frac{H_O}{p + \frac{2\beta T}{r_C^2}\left[\frac{r_S\sqrt{\frac{p}{D}} K_1\left(r_S\sqrt{\frac{p}{D}}\right)}{K_0\left(r_S\sqrt{\frac{p}{D}}\right)}\right]} \ (p >> R_J) \tag{12a}$$

$$\beta = 2\sum_{J=1}^{\infty} B_J^2 \tag{12b}$$

The series sum β reflects the partial penetration of the sandpack, in view of Equation (8c).

Hildebrand (1976) demonstrates that complex integration on the Bromwich contour, shown in Figure 4(a), inverts a transformed function with a branch point at the origin and no poles. The short term solution $h_{Short}(t)$ reduces to an integral of the transformed function $F_{Short}(p)$ along the

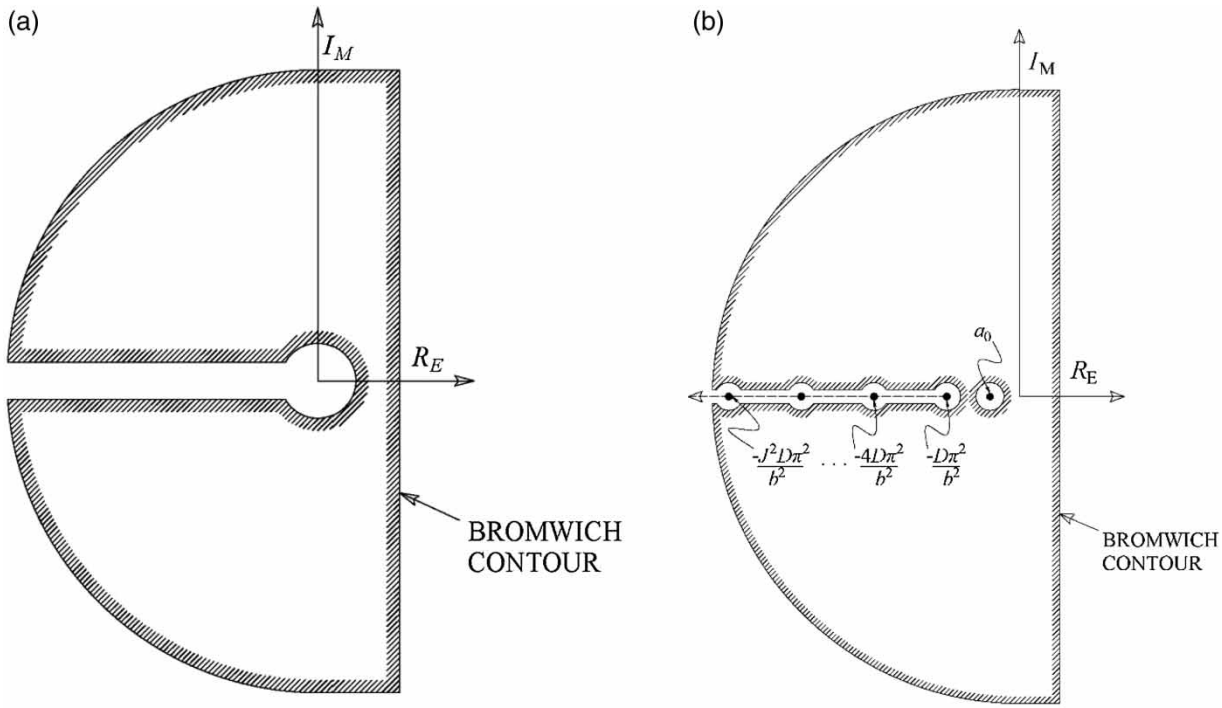

Figure 4 | Bromwich contours for Laplace transform inversion of (a) radial flow with branch point at origin and (b) cylindrical flow with pole and multiple branch points.

negative real axis -R of the Bromwich contour:

$$h_{Short}(t) = \frac{1}{2\pi i}\int_0^\infty e^{-tR}\left[F_{Short}\left(Re^{-i\pi}\right) - F_{Short}\left(Re^{i\pi}\right)\right]dR \tag{13a}$$

$$F_{Short}(p) = \frac{H_O}{p + \dfrac{2\beta T}{r_C^2}\left[\dfrac{r_S\sqrt{\dfrac{p}{D}}K_1\left(r_S\sqrt{\dfrac{p}{D}}\right)}{K_0\left(r_S\sqrt{\dfrac{p}{D}}\right)}\right]} \tag{13b}$$

Carslaw & Jaeger (1973) use Bessel function identities and a change of variables to invert Equation (13) for heat transfer:

$$u = r_S\sqrt{\frac{R}{D}} \tag{14a}$$

$$\frac{K_1\left(ue^{\pm\frac{i\pi}{2}}\right)}{K_0\left(ue^{\pm\frac{i\pi}{2}}\right)} = \frac{\frac{2}{\pi u} \mp i\left[J_1(u)J_0(u) + Y_1(u)Y_0(u)\right]}{[J_0(u)]^2 + [Y_0(u)]^2} \tag{14b}$$

$$J_0(u)Y_1(u) - Y_0(u)J_1(u) = -\frac{2}{\pi u} \tag{14c}$$

$$F_{Short}\left(Re^{\pm i\pi}\right) = \frac{H_O r_C^2}{2\beta T u\left(-\dfrac{ur_C^2}{2\beta S r_S^2} + \dfrac{J_1(u)J_0(u) + Y_1(u)Y_0(u)}{[J_0(u)]^2 + [Y_0(u)]^2} \pm \dfrac{2i}{\pi u\left\{[J_0(u)]^2 + [Y_0(u)]^2\right\}}\right)} \tag{14d}$$

The N order Bessel functions of the first and second kind are J_N and Y_N. We substitute Equation (14d) into Equation (13a), take the complex conjugate, invoke Equation (14a), and so derive the short term solution for the present case:

$$h_{Short} = \frac{8H_O\beta S r_S^2}{\pi^2 r_C^2} \int_0^\infty \frac{\exp\left(-Dt\dfrac{u^2}{r_S^2}\right)}{u\left\{\left[uJ_0(u) - 2\beta S\dfrac{r_S^2}{r_C^2}J_1(u)\right]^2 + \left[uY_0(u) - 2\beta S\dfrac{r_S^2}{r_C^2}Y_1(u)\right]^2\right\}} du \ (t \to 0) \tag{15a}$$

$$S = \rho g \alpha b \tag{15b}$$

Equation (15b) defines the storativity S. We use 64 point Gauss quadrature (Bathe & Wilson 1976) to estimate the integral in Equation (15a), with coefficients provided by Abramowitz & Stegun (1972).

If the sandpack extends over the entire till, z_S is zero, L is b, β is one (Spiegel & Liu 1999), and Equation (15a) becomes identical to the Cooper *et al.* (1967) model for a fully penetrating, overdamped slug test in a confined aquifer. The coincidence suggests that most of the initial recovery of the head in the well is due to radial flow of stored groundwater released by soil near the sandpack. Leakage and cylindrical flow happen later.

A simple pole as the long term solution

Equation (11a) describes the complete solution, and the Bromwich contour integration is more complicated:

$$h_S(t) = \frac{1}{2\pi i}\int_{R_1}^\infty e^{-tR}\left[F\left(Re^{-i\pi}\right) - F\left(Re^{i\pi}\right)\right]dR + h_{Res}exp(a_0 t) \ (a_0 < 0) \tag{16a}$$

$$F(p) = \frac{H_O}{p + \dfrac{4T}{r_C^2}\sum_{J=1}^\infty \dfrac{B_J^2 r_S\left(\sqrt{p+R_J}\right)}{\sqrt{D}}\dfrac{K_1\left(\dfrac{r_S}{\sqrt{D}}\sqrt{p+R_J}\right)}{K_0\left(\dfrac{r_S}{\sqrt{D}}\sqrt{p+R_J}\right)}} \tag{16b}$$

Eigenfunctions in the Bessel function arguments put a simple pole a_0 and branch points along the negative real axis of the Bromwich contour, as shown in Figure 4(b). The modified Bessel functions in Equation (16b) have real arguments to the right of their branch points and imaginary arguments to the left, and the first branch point is the lower limit of integration.

The residue h_{Res} of the pole adds an exponential decay term to the solution:

$$h_{Res} = \frac{H_O}{1 + \dfrac{4T}{r_C^2}\sum_{J=1}^\infty B_J^2 \dfrac{d}{dp}\left[\dfrac{r_S}{\sqrt{D}}\sqrt{p+R_J}\dfrac{K_1\left(\dfrac{r_S}{\sqrt{D}}\sqrt{p+R_J}\right)}{K_0\left(\dfrac{r_S}{\sqrt{D}}\sqrt{p+R_J}\right)}\right]} \ (p = a_0) \tag{17}$$

Churchill *et al.* (1974) use a derivative of the denominator of Equation (16b) to evaluate the residue, and Hildebrand (1976) provides derivatives for the Bessel functions necessary to evaluate the residue series terms. Equation (2b) simplifies the result:

$$h_{Res} = \frac{H_O}{1 + 2S\left(\dfrac{r_S}{r_C}\right)^2\sum_{J=1}^\infty B_J^2\left\{\left[\dfrac{K_1\left(\dfrac{r_S}{\sqrt{D}}\sqrt{a_0+R_J}\right)}{K_0\left(\dfrac{r_S}{\sqrt{D}}\sqrt{a_0+R_J}\right)}\right]^2 - 1\right\}} \ (p = a_0) \tag{18}$$

The simple pole a_0 lies between the origin and the first branch point and is defined by a zero in the denominator

of Equation (16b). This establishes an implicit equation for the pole:

$$a_0 = -\frac{4T}{r_C^2}\sum_{J=1}^{\infty}\frac{B_J^2 r_S\sqrt{a_0+R_J}}{\sqrt{D}}\frac{K_1\left(\frac{r_S}{\sqrt{D}}\sqrt{a_0+R_J}\right)}{K_0\left(\frac{r_S}{\sqrt{D}}\sqrt{a_0+R_J}\right)}\ (R_1 > |a_0|) \tag{19a}$$

$$D = \frac{T}{S} \tag{19b}$$

The polar residue is the long term solution h_{Long} for the slug test, since the exponential term in the integrand of Equation (16a) eliminates the branch point integral from the solution as time increases:

$$h_{Long} = h_{Res}exp(a_0 t)\ (t \to \infty) \tag{20}$$

Spline function between the short and long term solutions

The exact inversion needed to derive the disturbed head h_S in the monitoring well requires complex contour integration of Equation (16a), which is difficult. A heuristic patching of long and short term solutions is adopted instead:

$$h_S = h_{Short}exp\left(-\frac{Dt}{L_{Match}^2}\right) + \left[1 - exp\left(-\frac{Dt}{L_{Match}^2}\right)\right]h_{Long} \tag{21}$$

The matching length L_{Match} is less than b, which characterizes the long term solution, and Equation (21) uses vertical diffusion across this length to interpolate between the asymptotic behavior. Figure 5 displays the patched solution for slug test AB, a –21 m slug test in a 2.5 cm radius monitoring well with an 11 cm radius sandpack 2.6 m long, resting on the lower boundary of a 30 m thick till layer of 0.00092 m^2/s diffusivity. The 4.8×10^{-16} m^2 permeability and 4.0×10^{-10} Pa^{-1} compressibility

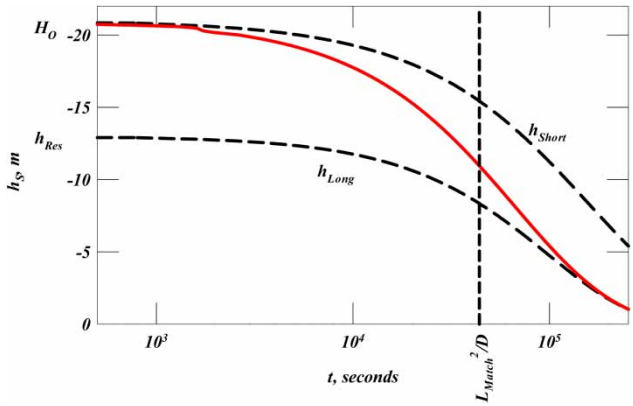

Figure 5 | Typical slug test prediction for a partially penetrating well (AB).

imply a –13 m polar residual. The matching length of 6.4 m shown in the figure creates an asymptotic departure from the short term solution at 1 hour and a long term approach about 3 days into the test.

Calibration

Figure 6 displays the first two orders of magnitude of the AB slug test, adding curves that illustrate graphical and programmed elements of model calibration. Figure 6(a) plots the AB data as symbols on a semilog plot of head against linear time. The concavity of the short term response confirms that storage initially affects the test, as suggested by Butler (1997). The slope and temporal intercept of the late term behavior offer graphical estimates of a_0 and h_{Res}. The former value of -1.0×10^{-5} s^{-1} and latter value of –13.0 m are cited in Table 2. Equations (18) and (19) yield an implicit equation for the hydraulic diffusivity in terms of the calibrated polar values:

$$\frac{-a_0}{\frac{H_0}{h_{Res}}-1} = \frac{2D}{r_S^2}\frac{\sum_{J=1}^{\infty}\frac{B_J^2 r_S\sqrt{a_0+R_J}}{\sqrt{D}}\frac{K_1\left(\frac{r_S}{\sqrt{D}}\sqrt{a_0+R_J}\right)}{K_0\left(\frac{r_S}{\sqrt{D}}\sqrt{a_0+R_J}\right)}}{\sum_{J=1}^{\infty}B_J^2\left\{\left[\frac{K_1\left(\frac{r_S}{\sqrt{D}}\sqrt{a_0+R_J}\right)}{K_0\left(\frac{r_S}{\sqrt{D}}\sqrt{a_0+R_J}\right)}\right]^2-1\right\}} \tag{22a}$$

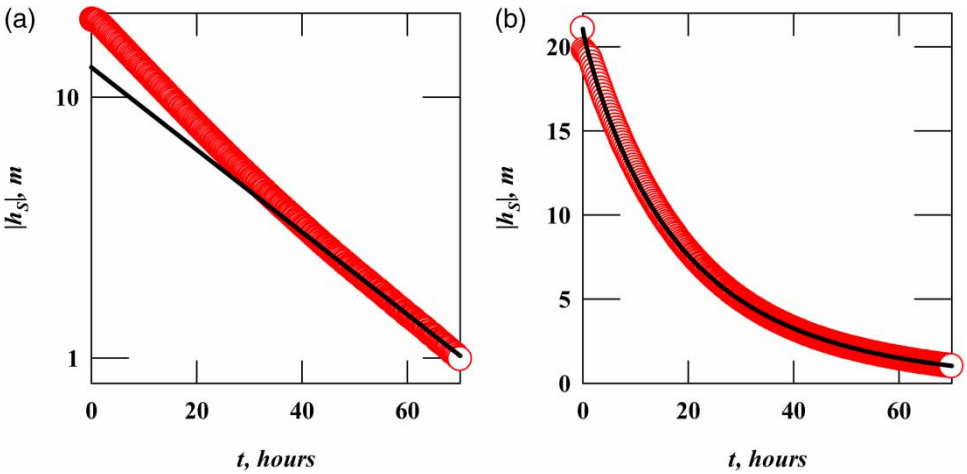

Figure 6 | Semilogarithmic (6a) and linear (6b) plots of observed (symbols) and graphically calibrated (curves) head, slug test AB.

$$D > -a_0\left(\frac{b}{\pi}\right)^2 \tag{22b}$$

The constraint of Equation (22b) requires that the pole lies to the right of the first branch point. Equation (22a) is iterated for a $-a_0/(H_O/h_{Res}-1)$ value of $1.6\times10^{-5}\ s^{-1}$, which converges to a D of $0.00092\ m^2/s$. The value is cited in Table 3. Equation (19a) yields the transmissivity ($1.1\times10^{-7}\ m^2/s$) with D and a_0 known:

$$T = -\frac{a_0 r_C^2}{4\sum_{J=1}^{\infty}\frac{B_J^2 r_S\sqrt{a_0+R_J}}{\sqrt{D}}\frac{K_1\left(\frac{r_S}{\sqrt{D}}\sqrt{a_0+R_J}\right)}{K_0\left(\frac{r_S}{\sqrt{D}}\sqrt{a_0+R_J}\right)}} \tag{23}$$

The storativity (0.00012) follows from Equation (19b), then the permeability ($4.8\times10^{-16}\ m^2$) and compressibility ($4.0\times10^{-10}\ Pa^{-1}$) from Equations (11b) and (15b), respectively. The long term behavior alone estimates intrinsic properties of the till, by graphical calibration.

The splined approximation Equation (21) of the complete solution then drives a Fibonacci search (Knuth 1973) for the matching length that minimizes the root mean square of the error defined by Equations (1) and (21). A value of 6.4 m yields an rms error of 2.7 cm, and the calibration plots as the line in Figure 6(b). The AB calibration is also plotted in Figure 5.

RESULTS

Calibrated parameter values

This graphical calibration of the long term solution is carried out for all 20 slug tests with the individual results summarized in Table 3 and the site averages in Table 1. The polar residues are from 5 to 90% of the slug amplitudes; thus an exponential decay constant does not describe the first two orders of magnitude of the recovery of head from the slug. The matching lengths vary from 2.4 to 20 m, with a 6.3 m arithmetic average. Figures 6(b) and 7 suggest that the approximation accurately patches the observed long and short term behavior of the test.

The long term behavior generates polar decay constants that range from -1.9×10^{-6} to $-1.3\times10^{-4}\ s^{-1}$, so that wells regain their ambient water levels within a few hours or a few days (Figure 2). The permeabilities vary from $1.0\times10^{-16}\ m^2$ in monitoring well EB to $9.3\times10^{-15}\ m^2$ in well BB with a (geometric) average value of $8.4\times10^{-16}\ m^2$. Table 1 confirms that the weathered till is over an order of magnitude more permeable than the unweathered till

Table 3 | Calibrated properties of unweathered till

Well	a_0, s^{-1}	h_{Res}, m	L_{Match}, m	D, m^2/s	S	T, m^2/s	k, m^2	α, Pa^{-1}
AB	-1.0×10^{-5}	−13	6.4	0.00092	0.00012	1.1×10^{-7}	4.8×10^{-16}	4.0×10^{-10}
AD	-2.1×10^{-5}	−4.0	7.0	0.0019	0.00021	3.9×10^{-7}	1.7×10^{-15}	7.0×10^{-10}
BB	-1.3×10^{-4}	−3.4	7.0	0.012	0.00018	2.1×10^{-6}	9.3×10^{-15}	6.1×10^{-10}
BC	-1.1×10^{-5}	−3.6	4.1	0.00098	0.00012	1.2×10^{-7}	5.2×10^{-16}	4.0×10^{-10}
CB	-8.3×10^{-6}	−3.5	4.1	0.00076	0.00012	9.4×10^{-8}	4.1×10^{-16}	4.2×10^{-10}
CD	-3.2×10^{-6}	−4.4	6.1	0.00029	0.00016	4.6×10^{-8}	2.0×10^{-16}	5.3×10^{-10}
DB	-3.1×10^{-5}	−3.8	3.7	0.0028	0.00014	3.8×10^{-7}	1.7×10^{-15}	4.6×10^{-10}
DC	-2.1×10^{-5}	−2.3	4.1	0.0019	0.00016	3.0×10^{-7}	1.3×10^{-15}	5.3×10^{-10}
EB	-1.9×10^{-6}	−14.0	5.3	0.00017	0.00013	2.3×10^{-8}	1.0×10^{-16}	4.5×10^{-10}
ED	-7.1×10^{-6}	−6.0	7.8	0.00065	0.00014	9.3×10^{-8}	4.1×10^{-16}	4.8×10^{-10}
GB	-3.8×10^{-5}	−0.90	2.4	0.0034	8.3×10^{-5}	2.8×10^{-7}	1.2×10^{-15}	2.8×10^{-10}
GC	-6.4×10^{-6}	−3.0	16	0.00059	0.00021	1.2×10^{-7}	5.4×10^{-16}	7.1×10^{-10}
HB	-5.0×10^{-5}	−2.0	3.4	0.0045	0.00016	7.3×10^{-7}	3.2×10^{-15}	5.5×10^{-10}
HC	-6.5×10^{-5}	−4.0	5.7	0.0060	0.00017	1.0×10^{-6}	4.6×10^{-15}	5.9×10^{-10}
IB	-9.7×10^{-6}	−3.5	3.0	0.00086	0.00014	1.2×10^{-7}	5.3×10^{-16}	4.6×10^{-10}
ID	-2.6×10^{-5}	−3.5	4.7	0.0024	0.00013	3.2×10^{-7}	1.4×10^{-15}	4.5×10^{-10}
LA	-7.6×10^{-6}	−15	5.7	0.00069	0.00014	9.4×10^{-8}	4.2×10^{-16}	4.6×10^{-10}
LD	-5.9×10^{-6}	−5.0	6.4	0.00054	0.00016	8.4×10^{-8}	3.7×10^{-16}	5.3×10^{-10}
TA	-1.4×10^{-5}	−5.0	19.9	0.0013	0.00015	2.0×10^{-7}	8.7×10^{-16}	5.1×10^{-10}
TD	-1.6×10^{-5}	−1.8	3.7	0.0015	0.00018	2.7×10^{-7}	1.2×10^{-15}	6.3×10^{-10}

beneath it. The transmissivities of Table 3 range from 2.3×10^{-8} to 2.1×10^{-6} m^2/s, with a (geometric) average (1.9×10^{-7} m^2/s) that is two orders of magnitude less than the fractured bedrock zone transmissivity cited in Table 1. The unweathered till is far less permeable than the underlying Dedham Granite, and the recharge boundary assumptions of the closed form analysis are justified at the site.

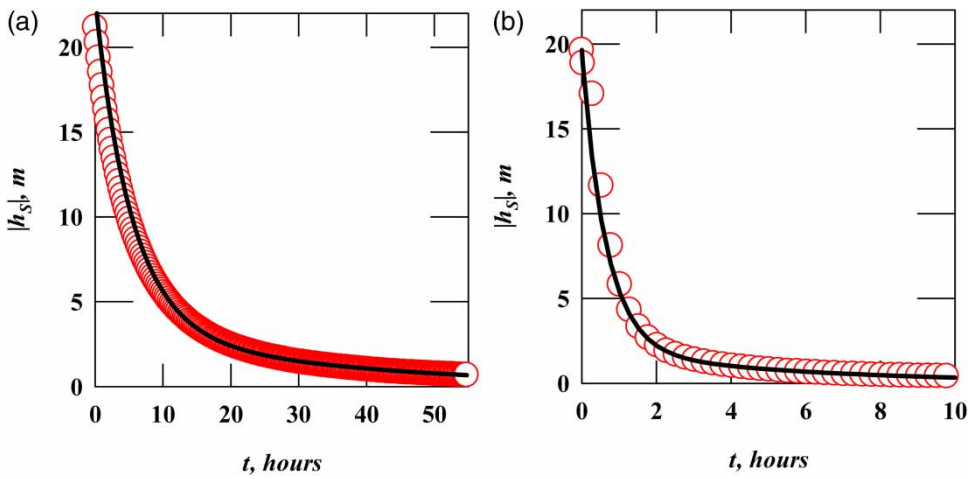

Figure 7 | Observed (symbols) and calibrated (curves) slug tests for impermeable (CB, (a)) and permeable (HB, (b)) monitoring wells.

The calibrated compressibilities range from 2.8×10^{-10} to 7.1×10^{-10} Pa^{-1}, with an arithmetic average of 5.1×10^{-10} Pa^{-1}. The values are an order of magnitude larger than the product of the 22% till porosity and the 4.4×10^{-10} Pa^{-1} compressibility of water (White 2011) and the 2×10^{-11} Pa^{-1} compressibility of unfractured Dedham Granite (Leet & Ewing 1932). Storage comes from the rearrangement of incompressible grains of the till in incompressible groundwater.

Bouwer & Rice (1976) and Cooper *et al.* (1967) comparisons

The poles compare directly to the exponential decay constant predicted by the Bouwer & Rice (1976) model for partially penetrating slug tests in unconfined aquifers:

$$-a_0 = \frac{2k_{BR}gL}{\nu r_C^2 \ln\left(\frac{r_e}{r_S}\right)} \tag{24}$$

The effective radius r_e depends on the well geometry and distance of the sandpack from the water table, and the impermeable lower boundary of the aquifer.

Figure 8 plots the permeability k_{BR} estimated by the Bouwer & Rice (1976) model against the Table 3 values for deep (circles) and shallow (squares) monitoring wells. The permeability of the deep slug tests is slightly overpredicted by the Bouwer & Rice (1976) model: k_{BR} is 12–30% higher than k with an average of 24%. The overprediction may be attributed in part to the assumption of an impermeable bottom boundary condition in the Bouwer & Rice (1976) analysis. Upward inflow from the Dedham Granite is responsible for some of the slug recovery as well as downward inflow from the till above the sandpack, and the former is not reflected in the effective radius curves relating to the numerical model of Bouwer & Rice (1976) to the simpler one dimensional approximation of the quasi-steady aquifer flow. By contrast, the permeability of the shallow tests is underpredicted by the Bouwer & Rice (1976) model: k_{BR} is 27–35% lower than k, with an average of 31%. The water table of Bouwer & Rice (1976) contributes more flow than the upper (zero disturbed head) recharge boundary of the present model.

Lukas *et al.* (2015) use Cooper *et al.* (1967) to calibrate the entire slug test for six of the deep till experiments. The flow field is purely radial in this approximation, and the confined aquifer thickness is equated to the sandpack length. The resulting compressibility estimates range from 2.6×10^{-10} to 2.4×10^{-4} Pa^{-1} for the slug tests under this assumption. Figures 5 and 9 help explain this behavior. The latter displays the data of experiment AB, plotted with the nondimensionalized, semilogarithmic format suggested by Cooper *et al.* (1967), but using the storativity and transmissivity calibrations of Table 3. Type curves from the Cooper *et al.* (1967) analysis are also shown in Figure 9. The progression from early to late term behavior, recovered by the heuristic spline curve of the cylindrically based Figure 5, implies a shift from a low compressibility Cooper *et al.* (1967) type curve to a much higher compressibility type curve. Our use of Cooper *et al.* (1967) as

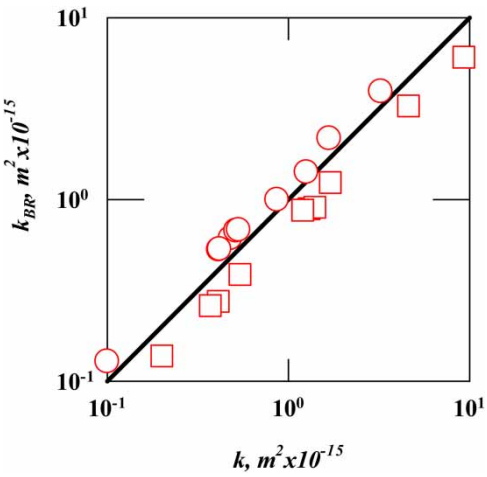

Figure 8 | Comparison of Bouwer & Rice (1976) and present calibrated permeability for slug tests in deep (circles) and shallow (squares) monitoring wells.

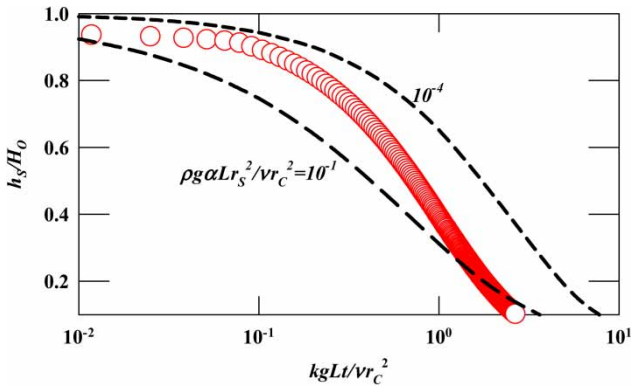

Figure 9 | Slug test AB data (symbols), nondimensionalized with calibrated values of Tables 2 and 3. Dotted lines are type curves from Cooper *et al.* (1967), using the sandpack thickness as the confined aquifer thickness.

a short term asymptote preserves the low compressibility calibration of the parameter. Late term behavior introduces vertical flow as the source of groundwater, rather than an increased release of storage from more compressible soil. The spline function of Figure 5 shifts the short term (type curve) behavior to an exponential late term prediction, rather than a higher compressibility type curve.

DISCUSSION

As a practical matter, the use of quasi-steady, radial slug test models to estimate permeability is confirmed by the cylindrical, closed form approach of the present analysis. Figure 8 establishes that Bouwer & Rice (1976) calibrations are well within an order of magnitude of the Table 3 permeabilities. Ostendorf *et al.* (2004) summarize Hvorslev (1951) calibrations of small amplitude slug tests at the site with an average permeability (1.4×10^{-15} m^2) that is close to the Table 1 value. Hyder *et al.* (1994) arrive at a similar conclusion through an extensive set of simulations. Our method does yield a tighter compressibility estimate than the radial models when the boundary conditions are met, however. The parameter is absent altogether from the Bouwer & Rice (1976) and Hvorslev (1951) models, while the Cooper *et al.* (1967) application precludes vertical flow and leakage. The radial models offer little insight into storage properties for partially penetrating slug tests in till.

Although the –20 m scale amplitude of the deep and –10 m scale amplitude of the shallow slug tests eliminate complicating effects of ambient transience on till property estimation, centimeter scale fluctuations can be used to advantage in simpler analyses. Ostendorf & DeGroot (2010) incorporate a linearly varying ambient head into a Bouwer & Rice (1976) analysis of a small amplitude slug test at a deep monitoring well (MA) at the Cohasset site; the 6.0×10^{-16} m^2 permeability compares favorably with the Table 3 values. The downward attenuation of storm scale disturbances observed at the G cluster implies a hydraulic diffusivity of 0.00043 m^2/s in the unweathered till (Ostendorf *et al.* 2004). This is less than the 0.0013 m^2/s site-wide value implied by Table 1, though it is the same order of magnitude. A site average compressibility of 3×10^{-9} Pa^{-1} and a site average permeability of 5.9×10^{-16} m^2 calibrate the response of the unweathered till to seasonal irrigation pumping of the Dedham Granite at an adjacent apartment complex (Ostendorf *et al.* 2015a).

CONCLUSIONS

A new semianalytical cylindrical model of a slug test in a partially penetrating monitoring well calibrates hydraulic properties of till bound by zero head recharge layers. A heuristic spline function patches initial and long term solutions together. Ten pairs of large amplitude slug tests in deep and shallow monitoring wells calibrate permeability and compressibility values at a till drumlin in eastern Massachusetts. The 8.4×10^{-16} m^2 permeability estimate is close to the value established by simpler radial slug test models at the site. The calibrated compressibilities of the 20 tests do not vary much from the site average value of 5.1×10^{-10} Pa^{-1} because the present analysis models vertical flow and recharge as a progressively more important groundwater source later in the experiment. Thus the low compressibility calibration accurately reflects the short term response to the test, when soil immediately near the sandpack flows radially into the well. Radial models rely on storage release for the groundwater throughout the test duration, and calibrate late term response with unrealistically high compressibilities as a consequence.

ACKNOWLEDGEMENTS

The Massachusetts Department of Transportation Highway Division funded this research under Interagency Service Agreement No. 73140 with the University of Massachusetts Amherst. The views, opinions, and findings contained in this paper are those of the authors and do not reflect MassDOT official views or policies. This paper does not constitute a standard, specification, or regulation.

REFERENCES

Abramowitz, M. & Stegun, I. A. 1972 *Handbook of Mathematical Functions*. National Bureau of Standards, Washington, DC.

Bathe, K. J. & Wilson, E. L. 1976 *Numerical Methods in Finite Element Analysis*. Prentice-Hall, Upper Saddle River, NJ.

Bouwer, H. & Rice, R. C. 1976 A slug test for determining the hydraulic conductivity of unconfined aquifers with completely or partially penetrating wells. *Water Resour. Res.* **12** (3), 423–428.

Brauchler, R., Hu, R., Vogt, T., Al-Halbouni, D., Heinrichs, T., Ptak, T. & Sauter, M. 2010 Cross well slug interference tests: an effective characterization method for resolving aquifer heterogeneity. *J. Hydrol.* **384** (1–2), 33–45.

Butler, J. J. 1997 *The Design, Performance, and Analysis of Slug Tests*. Lewis, Boca Raton, FL.

Carslaw, H. S. & Jaeger, J. C. 1973 *Conduction of Heat in Solids*. Oxford, New York, NY.

Churchill, R. V., Brown, J. W. & Verhey, R. F. 1974 *Complex Variables and Applications*. McGraw-Hill, New York, NY.

Cooper, H. H., Bredehoeft, J. D. & Papadopulos, I. S. 1967 Response of a finite diameter well to an instantaneous charge of water. *Water Resour. Res.* **3** (1), 263–269.

Goldsmith, R. 1991 Stratigraphy of the Milford-Dedham zone, eastern Massachusetts: an Avalonian terrane. *USGS Prof. Paper* **1366**, E1–E62.

Hantush, M. S. 1960 Modification of the theory of leaky aquifers. *J. Geophys. Res.* **65** (11), 3713–3725.

Hildebrand, F. B. 1976 *Advanced Calculus for Applications*. Prentice-Hall, Upper Saddle River, NJ.

Hvorslev, M. J. 1951 *Time Lag and Soil Permeability in Groundwater Observations. Bulletin 36*. Corps of Engineers, Vicksburg, MS.

Hyder, Z., Butler, J. J., McElwee, C. D. & Liu, W. 1994 Slug tests in partially penetrating wells. *Water Resour. Res.* **30** (11), 2945–2957.

Klinger, A. R. 1996 *Estimated Short Term Yields of and Quality of Groundwater in Stratified Drift Aquifer Areas in the Neponset River basin, Massachusetts. WRIR 93-4142*. USGS, Marlborough, MA.

Knuth, D. E. 1973 *The Art of Computer Programming Volume 3. Sorting and Searching*. Addison-Wesley, Reading, MA.

Leet, L. D. & Ewing, W. M. 1932 Velocity of elastic waves in granite. *J. Appl. Phys.* **2** (3), 160–173.

Lukas, W. G., DeGroot, D. J., Ostendorf, D. W. & Hinlein, E. S. 2015 Multiscale hydrogeologic characterization of a leaky till mantled fractured bedrock aquifer system. *Can. Geotech. J.* **52** (12), 1945–1955.

Neuman, S. P. & Witherspoon, P. A. 1969 Theory of flow in a confined two aquifer system. *Water Resour. Res.* **5** (4), 803–816.

Ostendorf, D. W. & DeGroot, D. J. 2010 Slug tests in the presence of background head trends. *Groundwater* **48** (4), 609–613.

Ostendorf, D. W., DeGroot, D. J., Shelburne, W. M. & Mitchell, T. J. 2004 Hydraulic head in a clayey sand till over multiple timescales. *Can. Geotech. J.* **41** (1), 89–105.

Ostendorf, D. W., Hinlein, E. S., Rotaru, C. & DeGroot, D. J. 2006 Contamination of groundwater by outdoor highway deicing agent storage. *J. Hydrol.* **326** (1), 109–121.

Ostendorf, D. W., Lukas, W. G. & Rotaru, C. 2015a Recharge and pumping hydraulics in a till drumlin above fractured bedrock (Massachusetts USA). *Hydrogeol. J.* **23** (4), 741–756.

Ostendorf, D. W., Lukas, W. G. & Hinlein, E. S. 2015b Closed form model of a damped slug test in a fractured bedrock borehole. *J. Hydrol.* **529**, 1116–1128.

Paradis, D. & Lefebvre, R. 2013 Single well interference slug tests to assess the vertical hydraulic conductivity of unconsolidated aquifers. *J. Hydrol.* **478**, 102–118.

Paradis, D., Gloaguen, E., Lefebvre, R. & Giroux, B. 2015 Resolution analysis of tomographic slug test head data: two dimensional radial case. *Water Resour. Res.* **51**, 2356–2376.

Sakata, Y., Imai, T., Ikeda, R. & Nishigaki, M. 2015 Analysis of partially penetrating slug tests in a stratified formation by alternating piezometer and tube methods. *J. Hydrol.* **528**, 385–396.

Spiegel, M. R. & Liu, J. 1999 *Mathematical Handbook of Formulas and Tables*. McGraw-Hill, New York, NY.

van der Kamp, G. 2001 Methods for determining the in situ hydraulic conductivity of shallow aquitards – an overview. *Hydrogeol. J.* **9** (1), 5–16.

Wang, Q., Zhan, H. & Wang, Y. 2015 Non-Darcian effect on slug test in a leaky confined aquifer. *J. Hydrol.* **527**, 747–753.

White, F. M. 2011 *Fluid Mechanics*. McGraw-Hill, New York, NY.

Yang, L., Wang, X. S. & Jiao, J. J. 2015 Numerical modeling of slug tests with MODFLOW using equivalent well blocks. *Groundwater* **53** (1), 158–163.

Yeh, H. D., Chen, Y. J. & Yang, S. Y. 2008 Semianalytical solution for a slug test in partially penetrating wells including the effect of finite thickness skin. *Hydrol. Proc.* **22**, 3741–3748.

Zlotnik, V. 1994 Interpretation of slug and packer tests in anisotropic aquifers. *Groundwater* **32** (5), 761–766.

First received 19 August 2015; accepted in revised form 7 February 2016. Available online 9 March 2016